POLITECNICO DI TORINO
Repository ISTITUZIONALE

Plant layout and pick-and-place strategies for improving performances in secondary packaging plants of food products

Original
Plant layout and pick-and-place strategies for improving performances in secondary packaging plants of food products / Comba, L., Belforte, G., Gay, P.. - In: PACKAGING TECHNOLOGY AND SCIENCE. - ISSN 0894-3214. - STAMPA. - 26:6(2013), pp. 339-354. [10.1002/pts.1984]

Availability:
This version is available at: 11583/2505134 since:

Publisher:
John Wiley & Sons, Ltd.

Published
DOI:10.1002/pts.1984

Terms of use:

This article is made available under terms and conditions as specified in the corresponding bibliographic description in the repository

Publisher copyright

(Article begins on next page)

25 November 2026

Insights of the DYDAS Project: The Use Case Energy

Ilaria Abbà [a], *Cristina* Becchio [b], *Stefano Paolo* Corgnati [c], *Paolo* Pasquali [d], *Maria Cristina* Pinto [e], *Elena* Roglia [f], *Sara* Viazzo [g].

[a] TEBE-IEEM Research Group, Energy Department, Politecnico di Torino, Torino, Italy, ilaria.abba@polito.it.

[b] TEBE-IEEM Research Group, Energy Department, Politecnico di Torino, Torino, Italy, cristina.becchio@polito.it.

[c] TEBE-IEEM Research Group, Energy Department, Politecnico di Torino, Torino, Italy, stefano.corgnati@polito.it.

[d] LINKS Foundation, Torino, Italy, paolo.pasquali@linksfoundation.com.

[e] TEBE-IEEM Research Group, Interuniversity Department of Regional and Urban Studies and Planning, Politecnico di Torino, Torino, Italy, mariacristina.pinto@polito.it.

[f] SDG11lab, Interuniversity Department of Regional and Urban Studies and Planning, Politecnico di Torino, Torino, Italy, elena.roglia@polito.it.

[g] TEBE-IEEM Research Group, Energy Department, Politecnico di Torino, Torino, Italy, sara.viazzo@polito.it

Abstract. In the current energy transition, Renewable Energy Sources are identified as key enablers for the achievement of the ambitious European target of climate neutrality by 2050; among them, solar and wind energy play a crucial role. The evolution of production, storage and end users' technologies goes hand in hand with the rapid development of the information sector, where High Performance Computing (HPC) infrastructures allow the exploitation of Internet of Things devices and Artificial Intelligence techniques. The use of HPCs in the energy field enables the use, processing and sharing of large volumes of energy data. The funded by the CEF TELECOM 2018 DYDAS (Dynamic Data Analytics Services) Project is carried out in the above-mentioned framework, aiming to create a collaborative platform, called DYDAS, that, using high-performing computers, will offer data, algorithms and data analysis services to a wide range of final users, both private and public. More specifically the paper will focus on the Use Case Energy, whose objective is to test and validate the DYDAS platform, by exploiting meteorological forecast techniques and using satellite information to facilitate and boost up the assessment of both energy demand and power production. Considering the strong dependency on resource availability, the localization of the resources and the related infrastructure is essential for an efficient and strategic energy planning. Therefore, the mix of traditional algorithms, climatic variables and remote sensing techniques represents an added value for supporting decision-makers in the energy planning processes at local and national scales, taking advantage of the geomatics instruments to visualize and monitor decision strategies. Given the role of electricity in the energy transition, the current paper deepens the Use Case Energy focusing on power generation from photovoltaic plants and on-shore and off-shore wind farms located in Italy. The aim of the use case is to estimate the potential local power production, by collecting information about technical features and geo-localization of real plants, and integrating them with georeferenced climatic variables, which can influence the electricity production (e.g., air temperature, solar irradiance, etc.).

Keywords. Renewable Energy Sources, High Performance Computing, remote sensing techniques, databases, geospatial data.
DOI: https://doi.org/10.34641/clima.2022.124

1. Introduction

In order to effectively tackle climate changes and speed up the energy transition process towards the 1.5°C goal as a limit for global temperature rising [1],[2], strong effort must be devoted to the efficient deployment of Renewable Energy Sources (RES). In particular, among the proposed solutions to achieve the target of a net zero energy system by 2050 [3], more than 90% concerns renewable energy [4]. Therefore, how to develop a strategic and efficient renewable planning process becomes a crucial step. According to this, the exploitation of geo-referenced data to assess geo-informed interventions plays an essential role, considering that different areas can do things differently, and thus understanding that the

Copyright ©2022 by the authors. This conference paper is published under a CC-BY-4.0 license.

energy transition is a geographically-constituted process [5]. To this end, the integration of different instruments able to combine a large volume of heterogeneous data and to extract valuable information can be exploited; in particular, using advanced Internet of Things (IoT) devices and Artificial Intelligence (AI) techniques. In this context, the DYDAS European project comes out to combine these aspects. In detail, DYDAS is a project funded by the CEF Telecom 2018 work program with the aim of contributing to the European data infrastructure by offering data, algorithms, processing and analysis services to different public and private user communities. The project is carried out by a consortium led by K2 Business partnering with ENEA, LINKS Foundation, Gmatics and ANCI Lazio. The platform DYDAS has been conceived as a marketplace platform that enables transactions for accessing data and services powered by High Performance Computing (HPC) and based on Big Data technologies, Machine Learning (ML), Artificial Intelligence and advanced data analytics. The platform consists of three main components: (i) data from different sources, algorithms and service providers; (ii) a supercomputing centre and the services it offers; (iii) various end-users from the public and private sectors. The adoption of a Geospatial Data Model and the use of interoperability rules enable large dataset integration and processing capabilities; this allows using geospatial information of different types and sources with data that are not intrinsically geo-referenced. Data are stored in a data lake defined by a Geospatial Data Architecture (GDA); the handling of all the datasets in a common geospatial fashion, through GDA, enables the application of HPC-AI-based services. To test the platform three Use Cases are developed: Maritime, Mobility and Energy.

Aiming to focus on the energy transition challenges and opportunities, especially with respect to the RES deployment, the Use Case Energy is suitable for this purpose and the current work will focus on its main features. Following the need of building up geo-informed solutions, it is mainly based on the use of meteorological forecast techniques and satellite information as a way to facilitate and boost up the assessment of both energy demand and renewable power production. In particular, being the renewable potential intrinsically based on geographical constraints, the strategic use of geo-referenced data, though the exploitation of Remote Sensing techniques and climate variables, as input for traditional algorithms and advanced data-processing systems, can support the energy planning processes, from a local to a national scale. The DYDAS Platform will provide access to a data domain able to offer an interesting mix of production and demand, in particular with respect to photovoltaic (PV) plants and on-shore and off-shore Wind Farms (WF) located in Italy. Specifically, it will allow the use of a data domain of interest, through its download and processing, and also of user-friendly visualization tools. In particular, (i) the data domain, (ii) the analysis domain and (iii) the communication domain are at the basis of an adequate geo-informed infrastructure [6]. As stressed by Fremouw et al. [7], in order to elaborate ad-hoc tools and support informed decisions combining physical-spatial problems with energy-environmental ones, the access to geo-referenced datasets is essential; improving their availability and quality is a crucial step towards their effective exploitation. Offering a structured spatial visualization of energy data means to support appropriate strategies and geo-informed interventions, then to identify priorities in energy planning, also through the selection of the most suitable locations [7]. The DYDAS Project, though the Use Case Energy, aims to address all the aforementioned challenges, making use of several instruments that, if correctly and efficiently combined, will allow to positively influence the energy transition process, paving the way for a more strategic allocation of RES. Specifically, being aware of the large volume of data involved in this type of analyses, the DYDAS platform makes use of HPC to deliver products that, through the integration of heterogeneous instruments and information, are able to share knowledge and to support decisions.

In this framework, the present paper aims to track and deepen the main steps leading to the elaboration of the hourly production profiles with respect to PV and wind technologies, in order to obtain geo-referenced data for renewable electricity generation to be matched with the local energy demand. Section 2 is dedicated to the main algorithms needed to obtain the production profiles; these algorithms, concerning respectively solar PV plants and wind farms, require certain data domains which are deepened in section 3. Section 4 reports some results of the work, and finally, section 5 summarizes the main outcomes and future perspectives of the project.

2. Research Methods

Wind and solar power are the most promising and widespread renewable sources in the world, being recognised as necessary and sustainable solutions to deal with the energy transition needs. Despite the high potentialities, the unpredictability of these sources represents a challenge for their integration in the energy system [8]. Therefore, to guarantee the correct operation of the power system and the correct demand-supply match, a prediction of wind farm and photovoltaic plant production is required. Akhter et al. [9] review the principal forecasting techniques for solar power previsions, classifying them according to the used method (physical, statistical or hybrid), forecasting horizon (intra-hour, intra-day or day ahead) and time step (minutes or hour according to the objective of the analysis). Considering that the objective of the current research is to provide at least a day ahead forecast, a physical model was used, since it performs better for short-/medium-term provisions, despite its high computational cost [10] (that in this case is mitigated

by the use of HPC), and an hourly time step was selected.

Both solar and wind sources are highly dependent on external weather conditions such as air temperature, solar radiation, wind velocity, as well as on local morphology of the ground. To consider all these aspects, the adopted methodology consists in the following steps: (i) identification of influencing climatic parameters; (ii) selection of proper algorithms from literature, able to take into account climatic and ground dependencies; (iii) identification of inputs and selection of relevant and complete databases for data collection; (iv) implementation of algorithms in a language suitable to be included and managed by the DYDAS platform.

In the following sub-sections, the main algorithms for the estimation of power production from wind farms and PV plants will be listed, while in Appendix A all the equations with the relative parameters involved in the calculation are reported.

2.1 Wind farms power production

Starting from wind farms, the assumption was that only horizontal axis wind turbines are used. In order to estimate the electric power output, it is necessary to calculate the mechanical power (P_{mech}) in W, generated by the turbine as in Eq.1 [11].

$$P_{mech} = \frac{1}{2} * \ c_p * \rho_{air}(h) * \pi * \frac{D^2}{4} * u^3(h, z_0) \quad (1)$$

Where c_p is the Power Coefficient and comes from producers' data (it must be lower than 16/27), h is the hub height. Then, as a rule of thumb, the height of the tower is almost 1.5 times the diameter of the rotor [12]. Therefore, since the height hub is a known parameter for each WF, the rotor diameter can be calculated as D=h/1.5. u and z_0 represent the wind speed [m/s] at the hub height and the roughness length of the soil [m], respectively.

If real data are not available, supposing air as a perfect gas, the following equations can be used to estimate the air density at the hub height. Equations expressing air pressure, temperature and density in function of the hub height are listed in Appendix A, according to [12],[13]. Moreover, there is a strong dependency also between wind speed (u), the height of the hub and the roughness of the ground (z_0), it can be expressed by Eq.2 [14].

$$u(h, z_0) = \ u_{ref} \frac{\ln\left(\frac{h}{z_0}\right)}{\ln\left(\frac{h_{ref}}{z_0}\right)} \quad (2)$$

It is well known that the wind turbine cannot exploit all the wind speeds, but there are some constrains, that are:

- Cut-in speed (u_c = 3-6 m/s), the wind turbine is not able to produce power until the wind reaches the cut-in speed [15];
- Rated speed (u_r = 12-15 m/s), before the rated speed the wind turbine tries to optimize the power output, while after this speed the regulation control starts to limit the power in order not to damage the turbine. Wind turbines are designed to deliver the maximum power at a speed of 12-15 m/s. Therefore, when the wind speed is higher, the power must be dissipated [15];
- Cut-off speed (u_f = 25 m/s), if the wind speed is higher than the cut of speed, the so-called thrust limit has been reached and the regulation control of the turbine shut-down the machine in order not to damage it [15].

According to this, the real mechanical power curve (P_{curve} in W) in function of wind speed follows Eq.3.

$$P_{curve} = P_r * \begin{cases} 0, & u < u_c \ \ or \ \ u > u_f \\ P_{asc}, & u_c < u < u_r \\ 1, & u_r < u < u_f \end{cases} \quad (3)$$

Where:

P_r is the rated power output [W], while $P_{asc} = P_{mech}/P_r$ is the turbine output as a percentage of P_{mech}. Finally, to convert the actual mechanical power (P_{curve}) into electric power (P_{el}), an efficiency of 40-45 % [14] must be used.

2.2 Photovoltaic plants power production

Moving to photovoltaic plants, the first step to calculate power production is the computation of solar radiation that arrives on the tilted plan of the panel (G_T). Solar radiation intensity depends not only on a set of meteorological parameters, but it is strictly influenced also by geometric features (e.g., solar angles, panel slope, tilt angle, etc.). All equations needed to compute the parameters involved in (G_T) are listed in Appendix A [16],[17],[18]. Moreover, Eq.4 allows to compute G_T for each hour of the year and for every location around the world.

$$G_T = G_{bn} * \cos(\theta) + G_{dh} * F_{c-s} + \rho * G_{th} * (1 - F_{c-s}) \quad (4)$$

$G_{bn,}$ G_{dh} and G_{th} represent the beam normal radiation, the diffuse horizontal radiation, and the total horizontal radiation [W/m^2], respectively. θ is the angle of incidence [°] of beam solar radiation on a surface whatever oriented and tilted; F_{c-s} is the collector-sky view factor, while ρ represents the albedo (or reflection coefficient) and are both dimensionless. Then, once knowing the total irradiance, the output DC power of the plant (P_{out_DC}) can be calculated, integrating equations [19] with technical data coming from PV panel datasheets.

$$P_{peak,plant} = \ \frac{G_T}{1000} * P_{N,plant} \quad (5)$$

$$T_c = T_a + \frac{[T_{c,NOCT} - T_{a,NOCT}]}{G_{NOCT}} * \frac{G_T}{1000} \quad (6)$$

$$P_{out_DC} = \ P_{peak,plant} - \left(\alpha_p * P_{peak,plant}\right) * \left(T_c - T_{c,STC}\right) \quad (7)$$

$P_{peak,plant}$ and $P_{N,plant}$ are the PV system peak power [kW] and the nominal power [kW]. T_c and $T_{c,STC}$ mean

the cell temperatures [°C] in operation and in Standard Test Condition (STC). T_a is the air temperature [°C], while $T_{c,NOCT}$, $T_{a,NOCT}$ and G_{NOCT} represent constant and predefined values concerning the panel cell temperature, the air temperature and the radiation on tilted surface in Nominal Operating Cell Temperature (NOCT) conditions. In particular, $T_{c,NOCT}$=45°C, $T_{a,NOCT}$=20°C and G_{NOCT}=800 W/m^2. Indeed, α_p is a correction factor, namely the temperature coefficient of maximum power of the solar cell.

2.2.1 Machine learning techniques for a proper detection of PV panels

Machine learning techniques were exploited for the purpose of using accurate datasets as input for the algorithms. Specifically, a trained model and high-resolution aerial images were used. Every time a new set of images is available the job can be run to update the census of active plants and estimate the power production over time. In particular, the accurate detection and delineation of PV panels was carried out by means of two similar deep learning approaches, namely Semantic Segmentation and Instance Segmentation. The former consists of classifying the whole image, pixel by pixel, in a predefined number of categories. The latter, after providing a detection box for every single panel, segments its contents to delineate the entity inside it, regardless of the category.

3. Applications

The Use Case Energy is applied to the Italian country, but the proposed methodology can be generalised and, in presence of consistent databases, can be implemented for any area of the World.

The Italian use case exploits data from different sources. In detail, climatic data, in the form of real time-products from the Atmospheric Model high-resolution 10-day forecast, come from European Centre for Medium-Range Weather Forecasts (ECMWF) [20] and Aeronautica Militare. Data are provided in GRIB format and 4 forecast runs per day (00:00; 06:00; 12:00; and 18.00) are performed with hourly steps to step 90 for all four runs. On the other hand, the spatial resolution is a 0.1° x 0.1° (almost 11.1 km) latitude/longitude grid, covering the whole Italian territory. The RES (wind farms and PV panels) location and features were collected from Gestore dei Servizi Energetici (GSE) datasets [21], while machine learning techniques were developed by LINKS Foundation (and then applied on CGR Spa Very High Resolution (VHR) Imagery [22].

The DYDAS platform adopts Apache Spark as processing engine [23]; all Spark jobs are written in Python as well as custom jobs submitted by remote users. Users can interact with the Platform exploiting a web interface running in Docker containers [24] in order to guarantee security and isolation by accessing only allowed resources and libraries.

In order to develop the Use Case Energy, a function is in charge to: (i) download the climate data from ECMWF [20]; (ii) calculate the required parameters from that data with an hourly time-step; and then (iii) assign the obtained spatial- and temporal-related values to each RES site to perform the energy production estimate.

Concerning the solar panel detection through machine learning techniques, a dataset of very high-resolution (VHR) images over two large areas of Piedmont, provided by CGR [22], was used. Over the same regions, LINKS Foundation also provided accurate manual annotations for more than 2000. To generate the input for the models, a pre-processing step was carried out independently for both modalities, with further tiling and filtering away every patch not containing useful information.

4. Results and discussion

Since the DYDAS project is currently ongoing, the platform is not yet implemented in its final and completed version; due to this, its potentiality cannot be fully exploited to extract valuable outputs, as it will be at the end of the project. In line with the above, this section is devoted to deepening some results of the process of solar panel delineation through aerial imagery. Using Semantic Segmentation, a class label was assigned to every pixel in the image according to three classes: (i) Background, for each object which does not represent a solar panel; (ii) Polycrystalline panels and (iii) Monocrystalline panels.

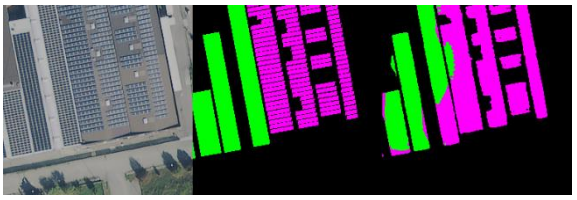


Fig. 1 - Example of Semantic Segmentation prediction.

Fig. 1 offers a visual output of Semantic Segmentation prediction. Specifically, from left to right a snapshot of Aerial image (RGB input), ground truth and, model prediction is shown, where green and magenta colors refer to Monocrystalline and Polycrystalline panels, respectively.

Concerning performances, the metric used to evaluate the accuracy of the Segmentation procedure was the Intersection over Union (IoU). This metric, varying between 0 and 1, is calculated as the ratio between the area of overlap (between the predicted bounding box and the ground-truth bounding box) and the area of union (the area encompassed by the predicted and the ground-truth bounding boxes). Therefore, the greater the overlapping area, the greater the accuracy is. According to this definition, the Background class, which is by far the most represented, performs very well, reaching an IoU = 0.9777. The second most accurate category is the Polycrystalline one (IoU =

0.9174), due to more frequent examples and its pattern was easier to notice from above. On the other hand, concerning Monocrystalline panels, their lower representation in terms of samples and the consequent more challenging detection, results in a lower performance of Monocrystalline (IoU = 0.7525). Generally speaking, the model performs very well on large solar plants, also thanks to a large panel surface, less background noise and simply a larger number of samples. Regarding the Instance Segmentation technique, considering the Average Precision with IoU at least of 0.5 the model can achieve a IoU of 0.8. Lower scores are typically associated with the extreme situation of solar plants that are very small or extremely large: smaller panels are more difficult to be delineated with precision, while larger panels cover a large portion of the image, making the detection step inherently more challenging. Therefore, in both cases (i.e., Semantic and Instance Segmentation), performances reach an IoU higher than 0.75 (considering Monocrystalline and Polycrystalline panels). Translating this score in percentage values, it means that at least 75% of the detections agree with human annotations, and the value can increase up to 88% in case of good conditions, especially for Polycrystalline panels. Therefore, it can be said that the outcomes of IoU calculation justify the use of Semantic Segmentation and Instance Segmentation techniques as a support tool for the identification of solar panels. Moreover, the final score can be negatively affected by the possible human error conflicting with the rightful detection of the model.

Concerning the power production by wind farms, the application of the algorithms presented in section 2.1 allowed to obtain the evolution of the electric power produced for the desired time horizon. In **Fig. 2** the forecast of the electric power output (P_{el}) of a wind farm located in Golfo di Manfredonia (Puglia, Italy) for the 2nd of March 2022 is shown through an hourly timestep; it is evident how the evolution of P_{el} follows the one of the wind speed along the day.

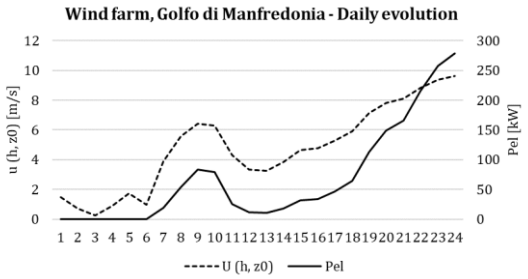


Fig. 2 - Example of daily evolution of wind speed and related electric power output for a wind farm.

Moreover, in **Fig. 3** the power production as a function of wind speed is reported. It highlights the cubic proportionality of the electric power output in the "usable range" of wind speed before the rated speed (as said in Eq. 3), and clearly shows that before the cut-in speed (3 m/s) the power output is zero since the wind speed is too low to produce power.

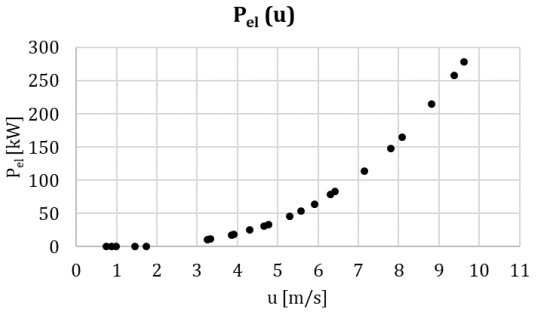


Fig. 3 - Daily wind power production as a function of wind speed.

5. Conclusions

Dealing with the opportunities and challenges of the energy transition requires strong efforts concerning the use of the appropriate instruments and datasets, specifically for an efficient deployment of RES. The DYDAS project, through the Use Case Energy, aims to create a marketplace enabling transactions for accessing data and services powered by HPC, to support geo-informed interventions for RES allocation. The integration of IoT devices and AI techniques makes the platform able to exploit advanced datasets, to optimize data processing and to deliver user-friendly outputs, supporting decisions and sharing knowledge. Focusing on the potentiality of the platform with respect to the prediction of renewable production, this paper introduced the appropriate algorithms for wind farm and PV plant production, to guarantee the correct operation of the power system and the correct demand-supply match. Specifically, the Use Case Energy is applied to the Italian territory, through the exploitation of different data sources and datasets. In addition, to deepen the integration of machine learning techniques in the platform structure, two deep learning approaches were investigated to obtain a more accurate detection of solar panels. These advanced models allow to improve the quality of input data used in the algorithms, obtaining a better accuracy.
Since the project is still ongoing, further work will be devoted to the validation of the production profiles and the implementation of user-friendly visualization tools to share geo-informed solutions. Moreover, future development of the DYDAS project will address the coupling of renewable production and electricity demand coming from residential and office buildings.

6. Acknowledgements

DYDAS is a project co-financed by the Connecting Europe Facility of the European Union, in particular by the CEF Telecom 2018 work program.

We thank the Italian "Servizio Meteorologico dell'Aeronautica Militare" for its collaboration in the provision of data.

The PhD research work of Ilaria Abbà and Maria Cristina Pinto has been financed by the Research Fund for the Italian Electrical System under the Contract Agreement between RSE S.p.A. and the Ministry of Economic Development - General Directorate for the Electricity Market, Renewable Energy and Energy Efficiency, Nuclear Energy in compliance with the Decree of April 16th, 2018.

7. Data access statement

The datasets generated during and/or analysed during the current study are not available because the DYDAS project is still ongoing, but the authors will make every reasonable effort to publish them in near future.

8. References

[1] UNFCCC. 2015. Key aspects of the Paris Agreement. https://unfccc.int/process-and-meetings/the-paris-agreement/the-paris-agreement/key-aspects-of-the-paris-agreement

[2] UN Climate Change Conference. 2021. COP 26 Glasgow Climate Pact. https://ukcop26.org/wp-content/uploads/2021/11/COP26-Presidency-Outcomes-The-Climate-Pact.pdf

[3] IEA. 2021. Net Zero by 2050, IEA, Paris https://www.iea.org/reports/net-zero-by-2050

[4] IRENA. 2021. World Energy Transitions Outlook. 1.5°C Pathway. https://irena.org/publications/2021/Jun/World-Energy-Transitions-Outlook

[5] Bridge G., Bouzarovski S., Bradshaw M., Eyred N. Geographies of energy transition: Space, place and the low carbon economy. Energy Policy. 2013;53:331-340.

[6] Calvert K., Pearce J. M., Mabee W. E. Toward renewable energy geo-information infrastructures: Applications of GIScience and remote sensing that build institutional capacity. Renewable and Sustainable Energy Reviews. 2013;18:416-429.

[7] Fremouw M., Bagaini A., De Pascali P. Energy Potential Mapping: Open data in support of Urban Transition Planning. energies. 2020;13(5):1264.

[8] Sun M., Feng C., Zhang J. Probabilistic solar power forecasting based on weather scenario generation. Applied Energy. 2020;266, 114823.

[9] Akhter M. N., Mekhilef S., Mokhlis H., Shah, N. M. Review on forecasting of photovoltaic power generation based on machine learning and metaheuristic techniques. IET Renewable Power Generation. 2019; 13(7):1009-1023.

[10] Feng C., Cui M., Hodge B. M., Zhang J. A data-driven multi-model methodology with deep feature selection for short-term wind forecasting. Applied Energy. 2017;190, 1245-1257.

[11] Mirzaei M., Göçmen T., Giebel G., Sorensen P., Poulsen N. Estimation of the possible power of a wind farm. IFAC Proceedings Volumes (IFAC-PapersOnline). 2014;19, 6782-6787.

[12] Manwell J.F., McGowan J.G., Rogers A.L. Wind Energy Explained: Theory, Design and Application. Wiley. 2010.

[13] Negash T., Möllerström E. Ottermo F. An Assessment of Wind Energy Potential for the Three Topographic Regions of Eritrea. Energies. 2020; 13(7), 1846.

[14] Wind Energy Department of Risø National Laboratory, Det Norske Veritas: Guidelines for Design of Wind Turbines. 2002.

[15] Chen K., Song M., He Z., Zhang X. Wind turbine positioning optimization of wind farm using greedy algorithm. Journal of Renewable and Sustainable Energy. 2013.

[16] Karafil A., Ozbay H., Kesler M., Parmaksiz H. Calculation of Optimum Fixed Tilt Angle of PV Panels Depending on Solar Angles and Comparison of the Results with Experimental Study Conducted in Summer in Bilecik, Turkey. 9th International Conference on Electrical and Electronics Engineering (ELECO), IEEE. 2015.

[17] Duffie J. A., Beckman W. A. Solar Engineering of Thermal Process. Fourth Edition. Wiley & Sons, Inc. 2013.

[18] Bottaccioli L., Patti E., Macii E., Acquaviva A. GIS-Based Software Infrastructure to Model PV Generation in Fine-Grained Spatio-Temporal Domain. IEEE Systems Journal. 2018; 12(3), 2832–2841.

[19] Mar A., Pereira P., Martins J. Energy Community Flexibility Solutions to Improve Users' Wellbeing. Energies. 2021;14(12), 3403.

[20] European Centre for Medium-Range Weather Forecasts (ECMWF).

https://www.ecmwf.int/en/about

[21] ATLAIMPIANTI. Gestore Servizi Energetici (GSE). https://www.gse.it/dati-e-scenari/atlaimpianti

[22] CGR SpA (Compagnia Generale Ripreseaeree) Very High Resolution (VHR) Imagery. https://www.cgrspa.com

[23] Apache Sparks. https://spark.apache.org

[24] Docker: Empowering App Development for Developers. https://www.docker.com/

Appendix A

This section lists all equation needed to compute power production Equations (reported in Section 2) for PV and WF plants, with a detailed description of each parameter involved.

Photovoltaic Plants

$$\delta = 23.45 * \sin\left(360 * \frac{284+n}{365}\right) \quad (8)$$

$$C = (n-1) * \frac{360}{365} \quad (9)$$

$$E = 229.2 * (0.00075 + 0.001868 * \cos(C) - 0.032077 * \sin(C) - 0.014645 * \cos(2C) - 0.04089 * \sin(2C)) \quad (10)$$

$$t_{solar} = t_{standard} - \frac{(L_{loc} - L_{ref})}{15} + \frac{E}{60} - DST \quad (11)$$

$$\omega = 15 * (t_{solar} - 12) \quad (12)$$

$$\cos(\theta_z) = \cos(\phi) * \cos(\delta) * \cos(\omega) + \sin(\phi) * \sin(\delta) \quad (13)$$

$$\cos(\gamma_s) = \frac{\cos(\theta_z) * \sin(\phi) - \sin(\delta)}{\sin(\theta_z) * \cos(\Phi)} \quad (14)$$

The slope of the panel changes daily, according to the following equation:

$$\beta = |\phi - \delta| \quad (15)$$

$$F_{c-s} = \frac{1+\cos(\beta)}{2} \quad (16)$$

$$\cos(\theta) = cos(\theta_z) * \cos(\beta) + sin\theta_z * \sin(\beta) * \cos(\gamma_s - \gamma) \quad (17)$$

Tab. 1 – Variables for PV production estimation.

Variables	Definition	Source	Dependencies
δ [°]	Solar declination. Positive towards North	Eq.8 – Cooper Formula [16]	Day of the year
n [day]	Ordinal day of the year	From 1 to 365	Day of the year
C [°]	Parameter for the calculation of E	Eq. 9	Day of the year
E [min]	Equation of time	Eq. 10	Day of the year
t_{solar} [h]	Time based on the apparent angular rotation of the Sun across the sky, assuming Solar time = 12 at Noon	Eq. 11	Hour of the day and location
$t_{standard}$ [h]	Time given by the local clock	Meteo-rological data	Hour of the day
L_{loc} [°]	Local longitude	GIS/ Meteorological data	Location
L_{ref} [°]	Longitude of the reference meridian for the local time zone	$L_{ref} = -15°$	Constant value for Italy
DST [-]	Daylight Saving Time ("ora legale")	DST = 1 when "ora legale" DST = 0 when "ora solare"	Day of the year
ϕ [°]	Latitude. Positive towards North	GIS/ Meteo-rological data	Location
ω [°]	Hour angle. Positive towards West	Eq.12 [16]	Hour of the day and location
θ_z [°]	Zenith angle	Eq.13 [17]	Hour of the day and location
γ_s [°]	Azimuth angle. Positive towards West	Eq.14 [16]	Hour of the day and location

β [°]	Tilt angle	Eq.15 [16]	Day of the year and Location
γ [°]	Surface azimuth	Assumed γ = 0° [16]	Constant
ρ [-]	Reflection coefficient, albedo	Assumed ρ = 0.23.	Constant
F_{c-s} [-]	Collector-sky view factor	Eq. 16 [17]	Day of the year and Location
θ [°]	Angle of incidence of beam solar radiation on a surface whatever oriented and tilted	Eq. 17 [17]	Hour of the day and location
G_{bn} [W/m²]	Beam normal radiation	Meteo-rological data	Hour of the day and location
G_{dh} [W/m²]	Diffuse horizontal radiation	Meteo-rological data	Hour of the day and location
G_{th} [W/m²]	Total horizontal radiation	Meteo-rological data	Hour of the day and location
G_T [W/m²]	Total radiation on the tilted surface	Eq.1 [18]	Hour of the day and location

Wind Farms

First of all, pressure and temperature in function of the hub height (h) must be calculated, through Eq.18 [12],[13] and Eq.19 [12], respectively.

$$Pressure_{air}(h) = 101.29 - (0.011837) * h + (4.793 * 10^{-7}) * h^2 \quad (18)$$

$$T_{air}(h) = T_{air} - 0.0066 * h \quad (19)$$

Then, using perfect gas equation density at the hub height can be computed (Eq. 20) [12],[13].

$$\rho_{air}(h) = 3.4837 * \frac{Pressure_{air}(h)}{T_{air}(h)} \quad (20)$$

Tab. 2 – Variables for WF production estimation.

Variables	Definition	Source	Dependencies
P_{mech} [W]	Mechanical power output	Eq.1 [11]	Hour of the day and location
$Pressure_{air}(h$ [Pa]	Pressure of the air at the hub height	Eq. 18 [12][13]	Hour of the day and location
T_{air} [°C]	Air temperature at ground level	Meteo-rological data	Hour of the day and location
$T_{air}(h)$ [°C]	Air temperature at hub height	Eq. 19 [12]	Hour of the day and location
$\rho_{air}(h)$ [kg/m³]	Air density at the hub height	Eq.20 [12][13]	Hour of the day and location
c_p [-]	Power coefficient	Producer data or assumption	Constant
u [m/s]	Wind speed at the hub height	Eq.5 [14]	Hour of the day and location
D [m]	Diameter of the rotor blade	Eq. 6 [12]	Location
h [m]	Height of the hub	Elaborations	Location
z_0 [m]	Roughness length of the soil	Producer data or assumption	Constant
u_{ref} [m/s]	Wind speed at the reference height	Meteo-rological data	Hour of the day and location
h_{ref} [m]	Reference height	10 m [14]	Constant